ELSEVIER

Metallation of PtRu$_5$(CO)$_{16}$(μ_6-C) by using bis(tri-t-butyl-phosphine) complexes of platinum and palladium

Richard D. Adams*, Burjor Captain, Wei Fu, Mark D. Smith

Department of Chemistry and Biochemistry and the USC Nanocenter, University of South Carolina, GRSC, 631 Sumter Street, Columbia, SC 29208, USA

Abstract

Pt(PBu$_3^t$)$_2$ and Pd(PBu$_3^t$)$_2$ react with PtRu$_5$(CO)$_{16}$(μ_6-C) (**4**) to yield the new cluster complexes, PtRu$_5$(CO)$_{16}$(μ_6-C)[Pt(PBu$_3^t$)] (**5**); PtRu$_5$(CO)$_{16}$(μ_6-C)[Pt(PBu$_3^t$)]$_2$ (**6**); PtRu$_5$(CO)$_{16}$(μ_6-C)[Pd(PBu$_3^t$)] (**7**) and PtRu$_5$(CO)$_{16}$(μ_6-C)[Pd(PBu$_3^t$)]$_2$ (**8**). All four complexes have been characterized crystallographically. Compounds **5** and **7** are structurally similar and contain a M(PBu$_3^t$) group bridging an Ru–Ru edge of the original cluster of **4**. Compounds **6** and **8** contain two M(PBu$_3^t$) groups. One group bridges an Ru–Ru edge as found in compounds **5** and **7**. The other M(PBu$_3^t$) group bridges one of the Pt–Ru edges of the original cluster of **4**. All four compounds can be viewed as M(PBu$_3^t$) adducts of **4** because no ligands were lost from **4** in the course of these addition reactions.
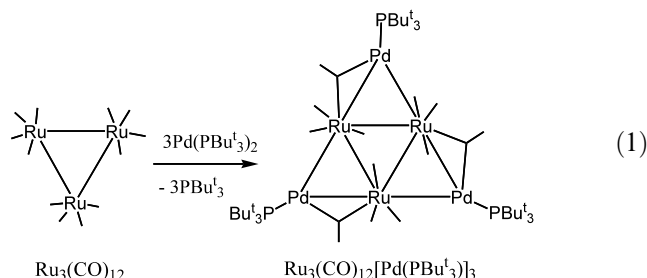© 2003 Elsevier B.V. All rights reserved.

Keywords: Ruthenium; Platinum; Palladium; Bimetallic clusters

1. Introduction

Mixed-metal clusters on supports have received great attention because of their superior catalytic properties [1,2]. It has been suggested that the presence of different metals in the proximity of a catalytically active site can lead to a higher reactivity and higher selectivity by synergistic effects [3]. Recently it has been shown that mixed-metal clusters are good precursors for the preparation of supported bimetallic nanoparticles [4–11] and supported heterogeneous catalysts [2]. Platinum–ruthenium and palladium–ruthenium mixed-metal clusters supported on mesoporous silica have been shown to exhibit high catalytic activity for certain hydrogenation reactions [1a,2].

We have recently demonstrated the ability of the compounds M(PBu$_3^t$)$_2$, M = Pd and Pt, to transfer

MPBu$_3^t$ groups to ruthenium–ruthenium bonds through the formation of a series of novel Lewis acid–base adduct complexes, e.g. (Eq. (1)) [12].


$$\text{Ru}_3(\text{CO})_{12} \xrightarrow[-3\text{PBu}^t_3]{3\text{Pd(PBu}^t_3)_2} \text{Ru}_3(\text{CO})_{12}[\text{Pd(PBu}^t_3)]_3 \qquad (1)$$

We have also prepared the adduct Ru$_5$(CO)$_{15}$(C)[PtPBu$_3^t$] (**1**) by the reaction of Pt(PBu$_3^t$)$_2$ with the pentaruthenium cluster Ru$_5$(CO)$_{15}$(μ_5-C) [13,14]. Compound **1** exists in solution as a mixture of isomers **1a** and **1b** that are in rapid equilibrium on the NMR timescale at room temperature. Related palladium adducts Ru$_5$(CO)$_{15}$(μ_6-C)[Pd(PBu$_3^t$)]$_n$ where $n = 1$ (compound **2**), $n = 2$ (com-

* Corresponding author. Tel.: +1-803-777-7187; fax: +1-803-777-6781.
E-mail address: adams@mail.chem.sc.edu (R.D. Adams).

pound **3**) were also obtained by the reaction of $Pd(PBu_3^t)_2$ with $Ru_5(CO)_{15}(\mu_5\text{-}C)$ and engage in similar dynamical processes [14].
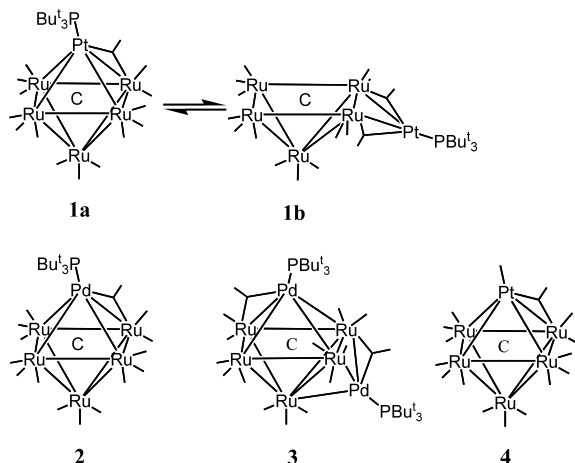
To examine the ability of Pt and Pd phosphine groups to add across metal–metal bonds further, we have now investigated the reaction of $Pt(PBu_3^t)_2$ and $Pd(PBu_3^t)_2$ with the platinum–ruthenium carbonyl cluster complex $PtRu_5(CO)_{16}(\mu_6\text{-}C)$ (**4**) [15]. A series of new adducts $PtRu_5(CO)_{16}(\mu_6\text{-}C)[M(PBu_3^t)]_n$, **5** and **6** where $M = Pt$ and $n = 1$ or 2, respectively, and **7** and **8**, where $M = Pd$ and $n = 1$ or 2, respectively, have been isolated and structurally characterized. These results are reported here.

2. Results and discussion

The reaction of **4** with an equimolar amount of $Pt(PBu_3^t)_2$ at room temperature afforded two new complexes, $PtRu_5(CO)_{16}(\mu_6\text{-}C)[Pt(PBu_3^t)]$ (**5**) in 28% yield and $PtRu_5(CO)_{16}(\mu_6\text{-}C)[Pt(PBu_3^t)]_2$ (**6**) in 21% yield. The yield of compound **6** was increased to 44%
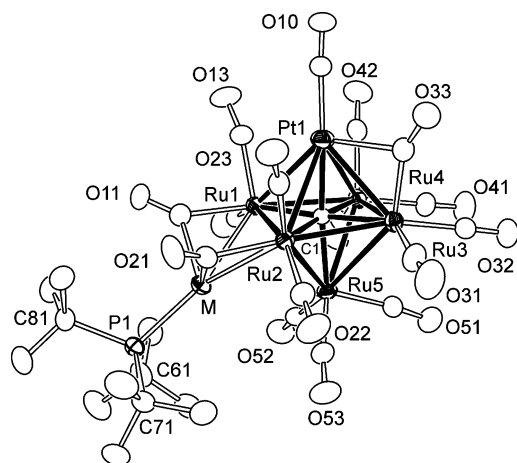

Fig. 1. An ORTEP diagram representing the molecular structures of compounds **5** and **7**, $PtRu_5(CO)_{16}(\mu_6\text{-}C)[M(PBu_3^t)]$, $M = Pt(2)$ and $Pd(1)$, respectively.
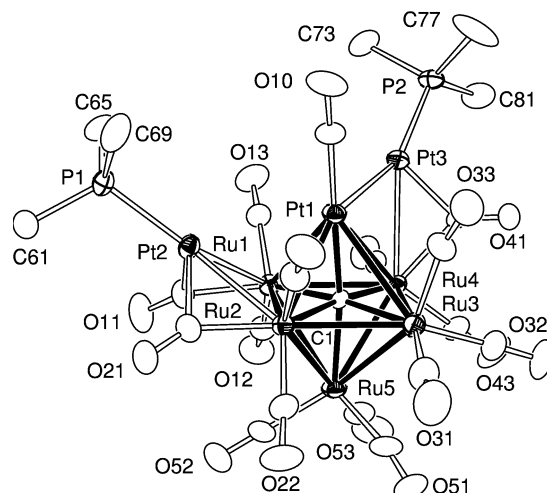

Fig. 2. An ORTEP diagram of the molecular structure of $PtRu_5(CO)_{16}(\mu_6\text{-}C)[Pt(PBu_3^t)]_2$ (**6**), showing 40% thermal ellipsoid probability. The carbon atoms on the ^{t}Bu groups have been omitted for clarity.

when an excess of $Pt(PBu_3^t)_2$ was used in the reaction. Both compounds were characterized by IR, ^{1}H- and ^{31}P-NMR, and single crystal X-ray diffraction analyses. The

Table 1
Selected intramolecular distances (Å) and angles (°) for compounds **5** and **7**

Compound **5**		Compound **7**	
Bond lengths			
Pt(1)–Ru(1)	2.8922(6)	Pt(1)–Ru(1)	2.9112(8)
Pt(1)–Ru(2)	2.9831(6)	Pt(1)–Ru(2)	2.9955(8)
Pt(1)–Ru(3)	2.7998(6)	Pt(1)–Ru(3)	2.7821(8)
Pt(1)–Ru(4)	2.9392(6)	Pt(1)–Ru(4)	2.9528(8)
Pt(2)–Ru(1)	2.7804(6)	Pd(1)–Ru(1)	2.8071(9)
Pt(2)–Ru(2)	2.8242(6)	Pd(1)–Ru(2)	2.8318(9)
Pt(2)–P(1)	2.3374(16)	Pd(1)–P(1)	2.393(2)
Ru(1)–Ru(2)	2.9587(7)	Ru(1)–Ru(2)	2.9541(9)
Ru(1)–Ru(4)	2.8638(7)	Ru(1)–Ru(4)	2.8584(10)
Ru(1)–Ru(5)	2.9569(7)	Ru(1)–Ru(5)	2.9615(9)
Ru(2)–Ru(3)	2.8950(7)	Ru(2)–Ru(3)	2.8919(10)
Ru(2)–Ru(5)	2.9082(7)	Ru(2)–Ru(5)	2.9007(10)
Ru(3)–Ru(4)	2.9474(8)	Ru(3)–Ru(4)	2.9477(10)
Ru(3)–Ru(5)	2.9276(7)	Ru(3)–Ru(5)	2.9365(10)
Ru(4)–Ru(5)	2.8241(7)	Ru(4)–Ru(5)	2.8226(10)
Pt(1)–C(1)	2.039(5)	Pt(1)–C(1)	2.050(7)
Ru(1)–C(1)	2.035(5)	Ru(1)–C(1)	2.038(8)
Ru(2)–C(1)	2.050(6)	Ru(2)–C(1)	2.053(8)
Ru(3)–C(1)	2.061(5)	Ru(3)–C(1)	2.051(8)
Ru(4)–C(1)	2.100(6)	Ru(4)–C(1)	2.093(8)
Ru(5)–C(1)	2.056(5)	Ru(5)–C(1)	2.061(8)
Bond angles			
Ru(1)–Pt(2)–Ru(2)	63.724(16)	Ru(1)–Pd(1)–Ru(2)	63.18(2)
Pt(2)–Ru(1)–Pt(1)	118.503(19)	Pd(1)–Ru(1)–Pt(1)	119.14(3)
Ru(3)–Pt(1)–Ru(1)	91.937(16)	Ru(3)–Pt(1)–Ru(1)	91.72(2)
Ru(5)–Ru(4)–Pt(1)	90.422(18)	Ru(5)–Ru(4)–Pt(1)	90.63(3)
Pt(1)–C(1)–Ru(5)	174.9(3)	Pt(1)–C(1)–Ru(5)	175.1(5)

Estimated standard deviations in the least significant figure are given in parentheses.

Table 2
Selected intramolecular distances (Å) and angles (°) for compounds **6** and **8**

Compound **6**		Compound **8**	
Bond lengths			
Pt(1)–Pt(3)	2.7311(4)	Pt(1)–Pd(2)	2.7837(5)
Pt(1)–Ru(1)	2.8729(7)	Pt(1)–Ru(1)	2.8058(5)
Pt(1)–Ru(2)	2.8500(7)	Pt(1)–Ru(2)	2.9209(5)
Pt(1)–Ru(3)	3.0372(8)	Pt(1)–Ru(3)	2.9118(5)
Pt(1)–Ru(4)	3.0096(7)	Pt(1)–Ru(4)	3.0338(5)
Pt(2)–Ru(1)	2.8234(7)	Pd(1)–Ru(1)	2.8154(5)
Pt(2)–Ru(2)	2.7892(7)	Pd(1)–Ru(2)	2.8362(5)
Pt(2)–P(1)	2.345(2)	Pd(1)–P(1)	2.4181(14)
Pt(3)–Ru(4)	2.8629(7)	Pd(2)–Ru(4)	2.8462(6)
Pt(3)–P(2)	2.284(2)	Pd(2)–P(2)	2.3922(15)
Ru(1)–Ru(2)	3.0544(9)	Ru(1)–Ru(2)	2.9534(5)
Ru(1)–Ru(4)	2.9165(9)	Ru(1)–Ru(4)	2.9394(6)
Ru(1)–Ru(4)	2.9165(9)	Ru(1)–Ru(5)	2.9849(6)
Ru(2)–Ru(3)	2.8502(9)	Ru(2)–Ru(3)	2.8743(6)
Ru(2)–Ru(5)	2.8515(9)	Ru(2)–Ru(5)	2.8959(6)
Ru(3)–Ru(4)	2.8904(10)	Ru(3)–Ru(4)	2.9310(6)
Ru(3)–Ru(5)	2.8794(10)	Ru(3)–Ru(5)	2.8953(6)
Ru(4)–Ru(5)	2.9079(9)	Ru(4)–Ru(5)	2.8449(6)
Pt(1)–C(1)	1.987(7)	Pt(1)–C(1)	2.041(5)
Ru(1)–C(1)	2.088(7)	Ru(1)–C(1)	2.035(4)
Ru(2)–C(1)	2.096(7)	Ru(2)–C(1)	2.085(4)
Ru(3)–C(1)	2.070(7)	Ru(3)–C(1)	2.064(4)
Ru(4)–C(1)	2.040(7)	Ru(4)–C(1)	2.085(4)
Ru(5)–C(1)	2.096(7)	Ru(5)–C(1)	2.063(5)
Bond angles			
Ru(2)–Pt(2)–Ru(1)	65.938(19)	Ru(1)–Pd(1)–Ru(2)	63.009(14)
Pt(1)–Pt(3)–Ru(4)	65.045(15)	Pt(1)–Pd(2)–Ru(4)	65.203(13)
Pt(2)–Ru(1)–Pt(1)	69.782(17)	Pt(1)–Ru(1)–Pd(1)	117.828(17)
Ru(1)–Pt(1)–Ru(3)	89.19(2)	Ru(1)–Pt(1)–Ru(3)	91.547(13)
Ru(5)–Ru(4)–Pt(1)	87.01(2)	Ru(5)–Ru(4)–Pt(1)	88.475(14)
Pt(1)–C(1)–Ru(5)	172.5(4)	Pt(1)–C(1)–Ru(5)	178.6(3)

Estimated standard deviations in the least significant figure are given in parentheses.

molecular structures of **5** and **6** are shown in Figs. 1 and 2, respectively. Selected bond distances and angles are listed in Tables 1 and 2, respectively. Because there was no loss of a CO ligand from **4**, compound **5** can be viewed most simply as a Pt(PBu$_3^t$) adduct of it. The structure of **5** consists of an octahedral cluster of six metal atoms; one platinum and five ruthenium atoms with a carbon atom in the center. A Pt(PBu$_3^t$) group, M = Pt(2) bridges the Ru(1)–Ru(2) edge of the octahedron and is displaced out of the Ru$_4$ square plane by 1.4863 (2) Å in the direction away from the platinum atom Pt(1). The PBu$_3^t$ ligand is terminally coordinated to the platinum atom. Two carbonyl ligands bridge from the PtRu$_5$ cluster to the platinum atom, one from Ru(1) and one from Ru(2). The Pt–Ru and Ru–Ru bond distances in the PtRu$_5$ cluster are similar to those found in **4** [15]. The Pt–Ru bond distances to the bridging Pt(PBu$_3^t$) group are 2.7804(6) and 2.8242(6) Å.

In compound **6** two Pt(PBu$_3^t$) groups have been added across two different metal–metal bonds of the

cluster **4**. As with **5**, there was no loss of CO from **4**, and so this compound can be viewed as a di-Pt(PBu$_3^t$) adduct of it. One Pt(PBu$_3^t$) group bridges the Ru(1)–Ru(2) edge of the Ru$_4$ square plane of the octahedron with two CO ligands from the PtRu$_5$ cluster bridging to the platinum atom, Pt(2). However, in contrast to that found in **5**, this Pt(PBu$_3^t$) group is displaced out of the Ru$_4$ plane toward Pt(1) by 1.3364(9) Å. The other Pt(PBu$_3^t$) group is a bridge across the Pt(1)–Ru(4) bond. There is only one bridging CO ligand to this platinum atom, Pt(3), which bridges the Pt(3)–Ru(4) bond. The Pt–Ru bond distances for the Pt(PBu$_3^t$) group on the Ru(1)–Ru(2) edge are similar to those found in compound **5**; 2.8234(7) and 2.7892(7) Å. The Pt(1)–Pt(3) bond distance is 2.7311(4) Å which is similar to that found in the compound Pt$_2$Ru$_4$(CO)$_{18}$, 2.6656(8) Å [16].

The two PBu$_3^t$ ligands in **6** are inequivalent in the solid state structure and so one would expect to see two resonances in the ^{31}P-NMR spectrum. However, at room temperature and even at −80 °C, only a single resonance is observed with ^{31}P–^{195}Pt couplings of $^1J_{Pt–P} = 6168$ Hz, $^3J_{Pt–P} = 158$ Hz. It is possible that the molecule has adopted a different structure in solution having equivalent PBu$_3^t$ groups, but it is also possible that the molecule is dynamically active on the NMR timescale and the Pt(PBu$_3^t$) groups are interconverting their sites. We have recently shown that that both Pt(PBu$_3^t$) and Pd(PBu$_3^t$) groups can migrate rapidly about the Ru$_5$(CO)$_{15}$(C) cluster [13,14].

The palladium compound, Pd(PBu$_3^t$)$_2$, also reacts with **4** at room temperature to yield the mono- and di-palladium adducts: PtRu$_5$(CO)$_{16}$(μ$_6$-C)[Pd(PBu$_3^t$)] (**7**) in 33% yield and PtRu$_5$(CO)$_{16}$(μ$_6$-C)[Pd(PBu$_3^t$)]$_2$ (**8**) in 35% yield. Both compounds were characterized by IR, ^{1}H- and ^{31}P-NMR, and single crystal X-ray diffraction analyses. Selected bond distances and angles are listed in Tables 1 and 2, respectively. The structure of compound **7** is analogous to that of **5**, and both compounds are isomorphous and isostructural in the solid state, see Fig. 1. Compound **7** consists of a PtRu$_5$ octahedral core with a carbon atom in the center and a Pd(PBu$_3^t$) group bridging the Ru(1)–Ru(2) edge on the Ru$_4$ square plane. The bridging Pd(PBu$_3^t$) group is displaced out of the Ru$_4$ square plane away from the Pt atom by 1.5843(10) Å as in compound **5**. Both Pd–Ru bonds are bridged by a CO ligand from the PtRu$_5$ cluster. The Pd(1)–Ru(1) and Pd(1)–Ru(2) bond distances are 2.8071(9) and 2.8318(9) Å, respectively.

The structure of compound **8** is similar to that of compound **6** with one Pd(PBu$_3^t$) group bridging the Ru(1)–Ru(2) edge on the Ru$_4$ square and the other Pd(PBu$_3^t$) group bridging the Pt(1)–Ru(4) edge. CO ligands bridge each of the Pd–Ru bonds. One CO ligand bridges the Pd(2)–Ru(4) bond. Unlike compound **6**
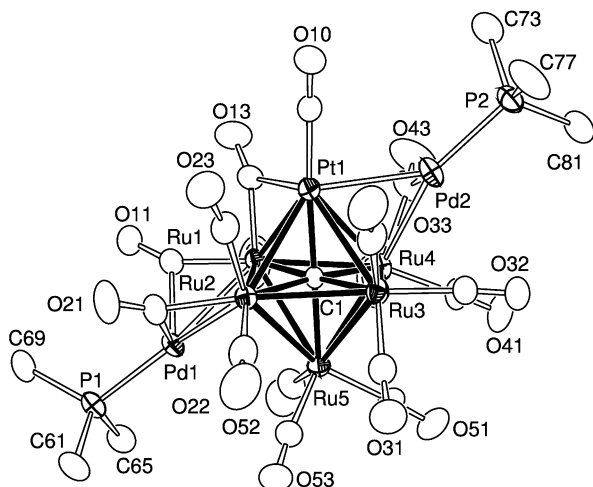
Fig. 3. An ORTEP diagram of the molecular structure of PtRu$_5$(CO)$_{16}$(μ_6-C)[Pd(PBu$^t_3$)]$_2$ (**8**), showing 40% thermal ellipsoid probability. The carbon atoms on the ^{t}Bu groups have been omitted for clarity.

where the Pt(PBu$^t_3$) group is displaced toward the Pt atom in the cluster, in **8** the edge bridging Pd(PBu$^t_3$) group on Ru(1)–Ru(2) is displaced away from the Pt atom by 1.5782(6) Å as found in **5** and **7**, see Fig. 3. The Pd–Ru and Pd–Pt bond distances are similar to those found in compounds **5**, **6** and **7**: Pd(1)–Ru(1) = 2.8154(5) Å, Pd(1)–Ru(2) = 2.8362(5) Å, Pd(1)–Pt(1) = 2.7837(5) Å.

Here again we have demonstrated the ability of Pt(PBu$^t_3$) and Pd(PBu$^t_3$) groups to add readily across metal–metal bonds and more interestingly across a hetero metal–metal bond. Metalation by these Pt(PBu$^t_3$) and Pd(PBu$^t_3$) groups should find their application in the synthesis of new bimetallic cluster complexes which have been shown to be good precursors to bimetallic nano-particles and to supported bimetallic catalysts.
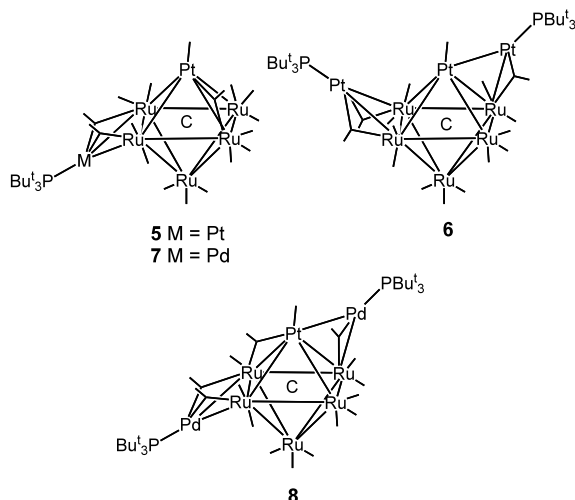
3. Experimental

3.1. General data

All reactions were performed under a nitrogen atmosphere. Reagent grade solvents were dried by the standard procedures and were freshly distilled prior to use. Infrared spectra were recorded on a Thermo Nicolet Avatar 360 FT-IR spectrophotometer. ^{1}H-NMR and ^{31}P-NMR were recorded on a Varian Inova 400 spectrometer operating at 399 and 168 MHz, respectively. ^{31}P-NMR spectra were externally referenced against 85% *ortho*-H$_3$PO$_4$. Elemental analyses were performed by Desert Analytics (Tucson, AZ). Bis(tri-*tert*-butyl phosphine)platinum(0), Pt(PBu$^t_3$)$_2$, and Bis(tri-*tert*-butyl phosphine)palladium(0), Pd(PBu$^t_3$)$_2$, were obtained from Strem and were used without further purification. PtRu$_5$(CO)$_{16}$(μ_6-C), (**4**) was prepared according to the published procedures [15]. Product separations were performed by TLC in air on Analtech 0.25 and 0.5 mm silica gel 60 Å F_{254} glass plates.

3.2. Reaction of 4 with Pt(PBu$^t_3$)$_2$

21.0 mg of **4** (0.0181 mmol) was dissolved in 15 ml of CH$_2$Cl$_2$. 11.0 mg of Pt(PBu$^t_3$)$_2$ (0.0183 mmol) was then added and the reaction mixture was stirred at room temperature (r.t.) for 10 min. Within a minute the color of the solution turned from red to dark red. The solvent was removed in vacuo and the residue was dissolved in CH$_2$Cl$_2$ and separated by TLC using a 4:1 hexane–methylene chloride solvent mixture. The compounds eluted in the following order were: Ru$_5$(CO)$_{15}$(μ_5-C)[Pt(PBu$^t_3$)] (light brown band, 4.0 mg, 16%), **2**; PtRu$_5$(CO)$_{16}$(μ_6-C)[Pt(PBu$^t_3$)] (grey–brown band, 8.0 mg, 28%), **5**; PtRu$_5$(CO)$_{16}$(μ_6-C)[Pt(PBu$^t_3$)]$_2$ (dark-brown band, 7.5 mg, 21%), **6**. Spectral data for **5**: IR ν_{CO} (cm^{-1} in CH$_2$Cl$_2$): 2086 (m), 2057 (s, sh), 2039 (vs), 1993 (w, sh), 1869 (w, br), 1793 (w, br). ^{1}H-NMR (CDCl$_3$): δ = 1.54 ppm (d, 27H, CH$_3$, $^3J_{P-H}$ = 13 Hz). ^{31}P{^{1}H} (CD$_2$Cl$_2$): δ = 116.8 ppm ($^1J_{Pt-P}$ = 6189 Hz, $^3J_{Pt-P}$ = 165 Hz). Anal. Calc. C, 22.34; H, 1.73; Found: C, 22.09; H, 1.74%. Spectral data for **6**: IR ν_{CO} (cm^{-1} in CH$_2$Cl$_2$): 2070 (m), 2035 (s), 2024 (sh), 1844 (w, br), 1817 (w, br), 1785 (w, br). ^{1}H-NMR (CDCl$_3$): δ = 1.53 ppm (d, 54H, CH$_3$, $^3J_{P-H}$ = 13 Hz). ^{31}P{^{1}H} (CDCl$_3$): δ = 117.1 ppm ($^1J_{Pt-P}$ = 6168 Hz, $^3J_{Pt-P}$ = 158 Hz). Anal. Calc. C, 25.18; H, 2.76; Found C 25.30, H 2.59%.

3.3. Improved yield of 6

12.2 mg of **4** (0.0105 mmol) was dissolved in 15 ml of CH$_2$Cl$_2$ to which 19.0 mg of Pt(PBu$^t_3$)$_2$ (0.0317 mmol)

was added. The reaction mixture was stirred at r.t. for 15 min after which the solvent was removed in vacuo. The reaction mixture was then separated by TLC using a 3:1 hexane–methylene chloride solvent mixture to yield 9.0 mg (44%) of **6**.

3.4. Reaction of **4** with $Pd(PBu_3^t)_2$

11.0 mg of **4** (0.0155 mmol) was dissolved in 15 ml of CH_2Cl_2 to which 9.0 mg of $Pd(PBu_3^t)_2$ (0.0176 mmol) was added. The color of the solution turned immediately from red to dark red. The reaction mixture was stirred at r.t. for 10 min, and the solvent was then removed in vacuo. The products were separated by TLC using a 4:1 hexane–methylene chloride solvent mixture. The compounds eluted in the following order were: $Ru_5(CO)_{15}(\mu_5-C)[Pd(PBu_3^t)]$ (light brown band, 2.1 mg, 11%), **3**; $PtRu_5(CO)_{16}(\mu_6-C)[Pd(PBu_3^t)]$ (brown band, 7.5 mg, 33%), **7**; $PtRu_5(CO)_{16}(\mu_6-C)[Pd(PBu_3^t)]_2$ (dark-brown band, 9.6 mg, 35%), **8**. Spectral data for **7**: IR ν_{CO} (cm^{-1} in CH_2Cl_2): 2087 (m), 2057 (sh), 2043 (vs), 1992 (w, sh), 1869 (w, br), 1823 (w, br). ^{1}H-NMR (CDCl$_3$): $\delta = 1.49$ ppm (d, 27H, CH$_3$, $^3J_{P-H} = 12$ Hz). ^{31}P{^{1}H} (CDCl$_3$): $\delta = 85.8$ ppm ($^3J_{Pt-P} = 150$ Hz). Spectral data for **8**: IR ν_{CO} (cm^{-1} in CH_2Cl_2): 2073 (m), 2037 (s), 2027 (sh), 1869 (w, br), 1815 (w, br). ^{1}H-NMR (CDCl$_3$): $\delta = 1.48$ ppm (d, 54H, CH$_3$, $^3J_{P-H} = 13$ Hz). ^{31}P{^{1}H} (CDCl$_3$): $\delta = 85.5$ ppm ($^3J_{Pt-P} = 149$ Hz).

3.5. Crystallographic analysis

Dark red crystals of **5**, **6** and **7** suitable for diffraction analysis were all grown by slow evaporation of solvent from solutions in hexane–methylene chloride solvent mixtures at 5 °C. Dark red crystals of **8** were grown by slow evaporation of solvent from solutions in hexane–methylene chloride solvent mixtures at r.t. Each data crystal was glued onto the end of thin glass fiber. X-ray intensity data were measured using a Bruker SMART APEX CCD-based diffractometer using Mo–K$_\alpha$ radiation ($\lambda = 0.71073$ Å). The raw data frames were integrated with the SAINT+ program by using a narrow-frame integration algorithm [17]. Correction for the Lorentz and polarization effects were also applied by SAINT. An empirical absorption correction based on the multiple measurement of equivalent reflections was applied by using the program SADABS. All four structures were solved by a combination of direct methods and difference Fourier syntheses, and refined by full-matrix least-squares on F_2, by using the SHELXTL software package [18]. Crystal data, data collection parameters, and results of the analyses for compounds **5** and **6** are listed in Table 3. For compounds **7** and **8** these data are listed in Table 4.

Compounds **5** and **7** are isomorphous and crystallized in the triclinic crystal system. The space group $P\bar{1}$ was

Table 3
Crystallographic data for compounds **5** and **6**

	5	**6**
Empirical formula	$Pt_2Ru_5PO_{16}C_{29}H_{27}$	$Pt_3Ru_5P_2O_{16}C_{41}H_{54}$
Formula weight	1558.01	1955.40
Crystal system	Triclinic	Monoclinic
Space group	$P\bar{1}$ (#2)	$P2_1/n$ (#14)
Lattice parameters		
a (Å)	9.1196 (8)	17.7888 (9)
b (Å)	13.9930 (12)	12.5139 (6)
c (Å)	15.8289 (14)	25.0125 (12)
α (°)	81.243 (2)	90
β (°)	85.688 (2)	102.4040 (10)
γ (°)	72.605 (2)	90
V (Å^3)	1904.1 (3)	5438.0 (5)
Z value	2	4
ρ_{calc} (g cm^{-3})	2.717	2.388
μ (Mo–K$_\alpha$) (mm^{-1})	9.356	9.154
Temperature (K)	293	293
$2\Theta_{max}$ (°)	52.82	52.04
No. Obs. ($I > 2\sigma(I)$)	6473	9206
No. Parameters	487	622
Goodness of fit	0.959	1.100
Max. shift in cycle	0.001	0.002
Residuals [a]: R_1; wR_2	0.0310; 0.0658	0.0395; 0.0988
Absorption Correction	SADABS	SADABS
Max/min	0.562/0.372	1.000/0.651
Largest peak in final difference map (e$^-$ Å^3)	2.128	2.963

[a] $R = \Sigma_{hkl}(||F_{obs}| - |F_{calc}||)/\Sigma_{hkl}|F_{obs}|$; $R_w = [\Sigma_{hkl}w(|F_{obs}| - |F_{calc}|)^2/\Sigma_{hkl}wF_{obs}^2]^{1/2}$, $w = 1/\sigma^2(F_{obs})$; GOF $= [\Sigma_{hkl}w(|F_{obs}| - |F_{calc}|)^2/(n_{data} - n_{vari})]^{1/2}$.

assumed and confirmed by the successful solution and refinement of the structure. The structures were solved by a combination of direct methods and difference Fourier syntheses, and refined by full-matrix least-squares on F_2, using the SHELXTL software package [18]. All non-hydrogen atoms were refined with anisotropic displacement parameters. Hydrogen atoms were placed in geometrically idealized positions and included as standard riding atoms.

Compounds **6** and **8** both crystallized in the monoclinic crystal system. The space groups $P2_1/n$ and $P2_1/c$ for compounds **6** and **8**, respectively, were identified uniquely on the basis of the systematic absences observed during the collection of the intensity data. The structures were solved by a combination of direct methods and difference Fourier syntheses, and refined by full-matrix least-squares on F_2, using the SHELXTL software package [18]. All non-hydrogen atoms were refined with anisotropic thermal parameters. Hydrogen atoms were placed in geometrically idealized positions and included as standard riding atoms.

Table 4
Crystallographic data for compounds **7** and **8**

	7	8
Empirical formula	$PtRu_5PdPO_{16}C_{29}H_{27}$	$PtRu_5Pd_2P_2O_{16}C_{41}H_{54}$
Formula weight	1469.32	1778.02
Crystal system	Triclinic	Monoclinic
Lattice parameters		
a (Å)	9.0929 (6)	20.8252 (9)
b (Å)	14.0187 (10)	15.0476 (6)
c (Å)	15.7179 (11)	18.4420 (8)
α (°)	80.733 (1)	90
β (°)	85.986 (1)	109.563 (1)
γ (°)	72.694 (1)	90
V (Å^3)	1887.4 (2)	5445.5 (4)
Space group	$P\bar{1}$ (#2)	$P2_1/c$ (#14)
Z value	2	4
ρ_{calc} (g cm^{-3})	2.585	2.169
μ (Mo–K$_\alpha$) (mm^{-1})	6.214	4.669
Temperature (K)	296	296
$2\Theta_{max}$ (°)	52.80	56.64
No. Obs. ($I > 2\sigma(I)$)	6710	10302
No. Parameters	487	621
Goodness of fit	1.0311	1.041
Max. shift in cycle	0.001	0.001
Residuals [a]: R_1; wR_2	0.0449; 0.1239	0.0373; 0.0890
Absorption correction	SADABS	SADABS
Max/min	0.582/0.430	1.000/0.773
Largest peak in final difference map (e$^-$ Å^3)	3.274	2.103

[a] $R = \Sigma_{hkl}(||F_{obs}|-|F_{calc}||)/\Sigma_{hkl}|F_{obs}|$; $R_w = [\Sigma_{hkl}w(|F_{obs}|-|F_{calc}|)^2/\Sigma_{hkl}wF_{obs}^2]^{1/2}$, $w = 1/\sigma^2(F_{obs})$; $GOF = [\Sigma_{hkl}w(|F_{obs}|-|F_{calc}|)^2/(n_{data}-n_{vari})]^{1/2}$.

4. Supplementary material

X-ray crystallographic data in CIF format for compounds **5**–**8** has been deposited with the Cambridge Crystallographic Data Centre. The deposit numbers are CCDC 212518–212521. Copies of this information may be obtained free of charge from The Director, CCDC, 12 Union Road, Cambridge CB2 1EZ, UK (Fax: +44-1223-336033; e-mail: deposit@ccdc.cam.ac.uk or www: http://www.ccdc.cam.ac.uk).

References

[1] (a) J.M. Thomas, B.F.G. Johnson, R. Raja, G. Sankar, P.A. Midgley, Acc. Chem. Res. 36 (2003) 20;
(b) J.H. Sinfelt, Bimetallic Catalysts: Discoveries, Concepts and Applications, Wiley, New York, 1983;
(c) J.H. Sinfelt, Bifunctional Catalysis: Adv. Chem. Eng. 5 (1964) 37;
(d) J.H. Sinfelt, Sci. Am. 253 (1985) 90.
[2] (a) R. Raja, T. Khimyak, J.M. Thomas, S. Hermans, B.F.G. Johnson, Angew. Chem. Int. Ed. Engl. 40 (2001) 4638;
(b) S. Hermans, R. Raja, J.M. Thomas, B.F.G. Johnson, G. Sankar, D. Gleeson, Angew. Chem. Int. Ed. 40 (2001) 1211;
(c) R. Raja, G. Sankar, S. Hermans, D.S. Shephard, S. Bromley, J.M. Thomas, B.F.G. Johnson, T. Maschemeyer, Chem. Commun. (1999) 1571.
[3] (a) D.W. Goodman, J.E. Houston, Science 236 (1987) 403;
(b) M. Ichikawa, Adv. Catal. 38 (1992) 283;
(c) R.D. Adams, J. Organomet. Chem. 600 (2000) 1.
[4] N. Toshima, T. Yonezawa, New J. Chem. (1998) 1179.
[5] B.F.G. Johnson, Coord. Chem. Rev. 192 (1999) 1269.
[6] P.A. Midgley, M. Weyland, J.M. Thomas, B.F.G. Johnson, Chem. Commun. (2001) 907.
[7] M.S. Nashner, A.I. Frenkel, D. Somerville, C.W. Hills, J.R. Shapley, R.G. Nuzzo, J. Am. Chem. Soc. 120 (1998) 8093.
[8] M.S. Nashner, A.I. Frenkel, D.L. Adler, J.R. Shapley, R.G. Nuzzo, J. Am. Chem. Soc. 119 (1997) 7760.
[9] D.S. Shephard, T. Maschmeyer, B.F.G. Johnson, J.M. Thomas, G. Sankar, D. Ozkaya, W. Zhou, R.D. Oldroyd, R.G. Bell, Angew. Chem. Int. Ed. Engl. 36 (1997) 2242.
[10] R. Raja, G. Sankar, S. Hermans, D.S. Shephard, S. Bromley, J.M. Thomas, B.F.G. Johnson, Chem. Commun. (1999) 1571.
[11] D.S. Shephard, T. Maschmeyer, G. Sankar, J.M. Thomas, D. Ozkaya, B.F.G. Johnson, R. Raja, R.D. Oldroyd, R.G. Bell, Chem. Eur. J. 4 (1998) 1214.
[12] R.D. Adams, B. Captain, W. Fu, M.D. Smith, J. Am. Chem. Soc. 124 (2002) 5628.
[13] R.D. Adams, B. Captain, W. Fu, P.J. Pellechia, M.D. Smith, Angew. Chem. Int. Ed. 41 (2002) 1951.
[14] R.D. Adams, B. Captain, W. Fu, P.J. Pellechia, M.D. Smith, Inorg. Chem. 42 (2003) 2094.
[15] R.D. Adams, W. Wu, J. Cluster Sci. 2 (1991) 271.
[16] R.D. Adams, G. Chen, W. Wu, J. Cluster Sci. 4 (1993) 119.
[17] SAINT+ Version 6.02a. Bruker Analytical X-ray System, Inc, Madison, WI, USA, 1998.
[18] G.M. Sheldrick, SHELXTL Version 5.1, Bruker Analytical X-ray Systems, Inc, Madison, WI, USA, 1997.